

# Residual correlations between decay products of $\pi^0\pi^0$ and $p\Sigma^0$ systems

A.Stavinskiy<sup>a</sup>, K.Mikhailov<sup>a</sup>, B.Erazmus<sup>b</sup>, R.Lednicky<sup>c,d</sup>

<sup>a</sup>*Institute of Theoretical and Experimental Physics,*

*B. Chermushkinskaya 25, 117259, Moscow, Russia*

<sup>b</sup>*SUBATECH, UMR Univ., EMN, IN2P3/CNRS,*

*4 rue A.Kastler, 44307 Nantes, France*

<sup>c</sup>*Joint Institute for Nuclear Research,*

*Dubna, Moscow Region, 141980, Russia*

<sup>d</sup>*Institute of Physics ASCR, Na Slovance 2, 18221 Prague 8, Czech Republic*

Residual correlations between decay products due to a combination of both correlations between parents at small relative velocities and small decay momenta are discussed. Residual correlations between photons from pion decays are considered as a new possible source of information on direct photon fraction. Residual correlations in  $p\gamma$  and  $p\Lambda$  systems due to  $p\Sigma^0$  interaction in final state are predicted based on the  $p\Sigma^0$  low energy scattering parameters deduced from the spin-flavour  $SU_6$  model by Fujiwara et al. including effective meson exchange potentials and explicit flavour symmetry breaking to reproduce the properties of the two-nucleon system and the low-energy hyperon-nucleon cross section data. The  $p\gamma\Sigma^0$  residual correlation is concentrated at  $k^* \approx 70$  Mev/ $c$  and its shape and intensity appears to be sensitive to the scattering parameters and space-time dimensions of the source. The  $p\Lambda\Sigma^0$  residual correlation recovers the negative parent  $p\Sigma^0$  correlation for  $k^* > 70$  Mev/ $c$ . The neglect of this negative residual correlation would lead to the underestimation of the parent  $p\Lambda$  correlation effect and to an overestimation of the source size.

## I. INTRODUCTION

Due to the effects of quantum statistics (QS) and final state interaction (FSI), the momentum correlations of two or more particles at small relative velocities, i.e. at small relative momenta in their center-of-mass (c.m.) system, are sensitive to the space-time characteristics of the production processes on a level of fm =  $10^{-15}$  m. Consequently, these correlations are widely used as a correlation femtoscopy tool providing a unique information on the reaction mechanism which is hardly accessible by other means (see, e.g., recent reviews [1, 2]).

The momentum correlations of two particles with four-momenta  $p_1$  and  $p_2$  are studied with the help of the correlation function  $\mathcal{R}(p_1, p_2)$  which is usually defined as the ratio of the measured distribution of the three-momenta of the two particles to the reference one obtained by mixing particles from different events of a given class, normalized to unity at sufficiently large relative momenta. It can be also written as the ratio of the two-particle production cross section to the product of the single-particle ones

$$\mathcal{R}(\mathbf{p}_1, \mathbf{p}_2) = N \frac{d^6\sigma/d^3\mathbf{p}_1 d^3\mathbf{p}_2}{d^3\sigma/d^3\mathbf{p}_1 \cdot d^3\sigma/d^3\mathbf{p}_2}, \quad (1)$$

where  $N$  is the normalization factor which is sometimes taken weakly dependent on the relative momentum to account for the effect of possible non-femtoscopic correlations.

At a first glance, one can hardly expect any correlations between photons from the decays of different neutral pions. The spatial separation between such photons is of the order of  $10^6$  fm and the corresponding Bose-Einstein enhancement is extremely narrow and practically unobservable. Nevertheless, due to femtoscopic QS correlations between parent pions at small relative momenta as well as due to a small decay momentum, correlations between decay photons from different neutral pions should exist and have been experimentally observed [3, 4]. The small decay momentum guarantees that a small relative momentum between photons corresponds to a small relative momentum between parent pions. For this kinematic reason the QS correlation between neutral pions is transferred to decay photons, being however smeared due to randomly distributed directions of the decay three-momenta in the respective parent rest frames. We shall refer to such correlations as the residual ones (see also [3, 4, 5]).

The residual correlations are important not only for two-photon system. For example, the two-baryon correlations are also affected by residual correlations arising from the FSI and

QS correlations in the systems involving strange baryons since the decay momenta in their decays (e.g.,  $\Lambda \rightarrow p\pi^-$  or  $\Sigma^0 \rightarrow \Lambda\gamma$ ) are not so large to destroy the original correlations [5]. The relative importance of the residual correlations is however quite different for two-photon and two-baryon systems. Usually, the residual two-photon correlation almost completely dominates over the correlation of direct photons. The residual correlations in two-baryon and other systems become more and more important with the increasing collision energy due to increasing fraction of the produced strange particles. Their analysis is therefore an up-to-date task.

The residual correlations do not represent only the distorting effect which introduces additional systematic errors in correlation studies. We would like to pay attention to the fact (to our knowledge, for the first time) that the residual correlation itself is a valuable source of femtoscopic information.

## II. TWO-PHOTON CORRELATIONS

To study the residual correlations between photons ( $\gamma_{\pi^0}$ ) from neutral pion decays ( $\pi^0 \rightarrow \gamma\gamma$ ), we have assumed that the photons are produced either through these decays or "directly" (similar to the production of  $\pi^0$ 's) and generated neutral pions and direct photons ( $\gamma_D$ ) according to the same thermal-like momentum distribution

$$dN/dp \propto (p^2/E)\exp(-E/T_0), \quad (2)$$

where  $T_0 = 168$  MeV. Usually, there is the experimental threshold in the energy of detected photons. To take it into account we have rejected photons with  $E_\gamma < 80$  MeV. Such a cut increases the relative strength of the correlation of direct photons and modifies the relative strength and shape of residual correlations.

The fraction  $d = N(\gamma_D)/[N(\gamma_{\pi^0})+N(\gamma_D)]$  of direct photons was considered as a simulation parameter ( $d = 0, 5, 10, 20\%$ ). Only the QS correlation has been introduced by giving each simulated pair of neutral pions and direct (unpolarized) photons a weight (see, e.g., [7])

$$\begin{aligned} \mathcal{R}(\mathbf{p}_1, \mathbf{p}_2) &= 1 + \lambda \langle \cos(2\mathbf{k}^* \cdot \mathbf{r}^*) \rangle \\ &= 1 + \lambda \exp(-Q^2 r_0^2), \end{aligned} \quad (3)$$

where  $\mathbf{Q} = 2\mathbf{k}^*$  and  $\mathbf{r}^*$  are respectively the relative three-momentum of the two particles and spatial separation vector of their emitters in the two-particle rest frame;  $Q = \sqrt{-(p_1 - p_2)^2}$

for the considered equal-mass particles. The correlation strength parameter  $\lambda = 1$  for pions and  $1/2$  for unpolarized photons. A Gaussian  $\mathbf{r}^*$ -distribution with the same radius parameter  $r_0$  has been assumed in the averaging in Eq. (3) over the spatial separation  $\mathbf{r}^*$  for both pion and photon emitters:

$$d^3N/d^3\mathbf{r}^* \sim \exp(-\mathbf{r}^{*2}/4r_0^2). \quad (4)$$

This is a reasonable assumption for pions emitted with moderate transverse momenta. However, for photons, it leads to the non-realistic dependence of the correlation function on the outward component of the relative momentum in the longitudinally co-moving system (the component in the direction of the pair transverse momentum) due to the diverging Lorentz factor of the transformation to the two-photon rest frame at  $Q \rightarrow 0$ .

The two photon correlation functions corresponding to the radius parameter  $r_0 = 5$  fm and different direct photon fractions  $d$  are shown in Fig. 1 as functions of the relative momentum  $Q = 2k^*$  in the two-photon c.m. system assuming the ideal three-momentum resolution. The correlation functions are normalized to unity at  $Q \gg m_\pi$ . The peak at  $Q = m_{\pi^0}$  is related to photon pairs from the same  $\pi^0$ . The width of the peak in a real experiment depends on the three-momentum resolution. The residual correlations between decay photons from different  $\pi^0$ 's ( $\sim 81\%$  contribution for  $d = 0.1$ ) result in a smooth structure at  $Q < 0.17$  GeV. The uncorrelated background ( $\sim 18\%$  contribution for  $d = 0.1$ ) arises from  $\gamma_{\pi^0}\gamma_D$ -pairs. The pairs of direct photons ( $\sim 1\%$  contribution for  $d = 0.1$ ) provide the interference enhancement with a width of  $1/r_0 \sim 40$  MeV/ $c$ .

It is important that

- (i) the residual correlations represent a first order effect in the direct photon fraction  $d$ , to be compared with the second order effect of the interference correlations of direct photons;
- (ii) the residual correlation effect appears to be wider than the interference effect for  $\pi^0$ 's or direct photons.

As a result, for some combinations of a large source size  $r_0$  and a small direct photon fraction  $d$ , the direct photon interference is practically unobservable while the residual correlations can still be used to measure  $d$ .

It is important for the suggested method that the residual correlation function of decay photons (depending on the three-momentum spectrum of neutral pions, their correlations

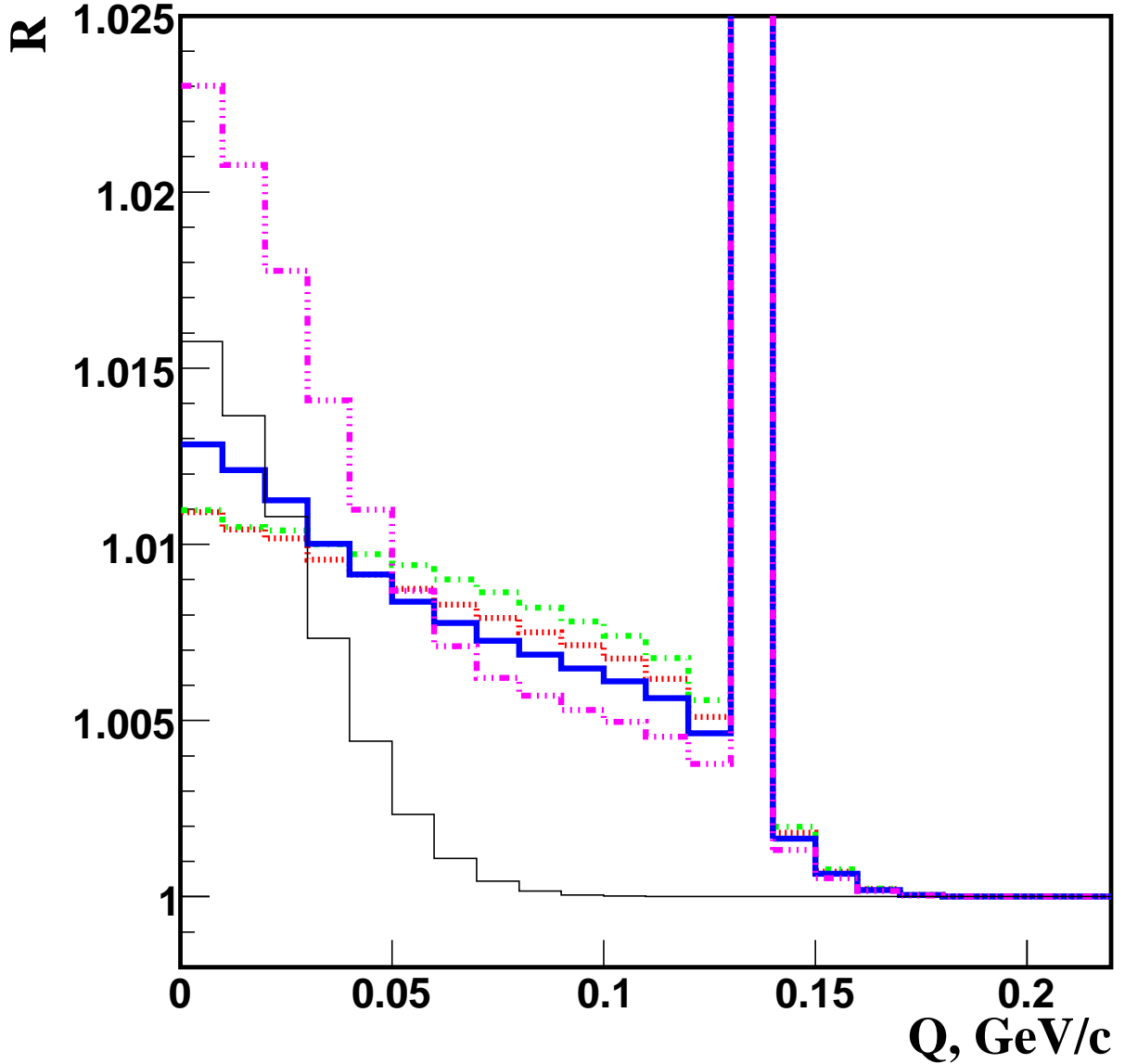


FIG. 1: The two-photon correlation functions calculated with the source size parameter  $r_0 = 5$  fm and different direct photon fractions  $d = N(\gamma_D)/[N(\gamma_{\pi^0}) + N(\gamma_D)]$ . The histograms correspond to  $d = 0$  (dashed-dotted), 0.05 (dotted), 0.10 (solid), 0.20 (dashed-triple-dotted). The thin solid histogram corresponds to  $d = 0.20$  and the residual correlation switched off.

and experimental conditions) could be predicted with sufficient accuracy. This is in contrast with the model-independent correlation measurement of the direct photon fractions in the experiment WA98 [4] exploiting the quadratic relation between the correlation strength parameter  $\lambda$  and the direct photon fraction (valid in sufficiently narrow interval of the three-

momenta of the selected photon pairs) and nearly constant residual correlation function of decay photons at  $Q < 90 \text{ MeV}/c$ .

### III. THE RESIDUAL CORRELATIONS IN $h\Lambda$ AND $h\gamma$ SYSTEMS INDUCED BY THE CORRELATIONS IN $h\Sigma^0$ SYSTEM

#### A. Kinematic considerations

Another interesting example of residual correlations are the correlations in  $h\Lambda$  and  $h\gamma$  systems (where  $h$  is a hadron) induced by the  $h\Sigma^0$  correlation at small relative  $h-\Sigma$  momenta  $2K$  in the  $h\Sigma^0$  c.m. system. One can express the momentum  $k^*$  of the hadron  $h$  in the  $h\Lambda$  or  $h\gamma$  c.m. system through the hadron three-momentum  $-\mathbf{K}$  as

$$k^* = m_h \left[ \frac{z^2 - m^2/m_h^2}{1 + m^2/m_h^2 + 2z} \right]^{1/2}$$

$$z = \frac{\omega_D(\omega_h\omega_\Sigma + K^2)}{m_\Sigma m_h^2} + \frac{p_D K(\omega_h + \omega_\Sigma)}{m_\Sigma m_h^2} \zeta, \quad (5)$$

where  $p_D = 74 \text{ MeV}/c$  is the decay momentum in the decay  $\Sigma^0 \rightarrow \Lambda\gamma$ ,  $m$  is the mass of the decay particle (a proton or a photon),  $\omega_D = (m^2 + p_D^2)^{1/2}$  is the corresponding decay energy,  $\omega_i = (m_i^2 + K^2)^{1/2}$  are the energies of the particles  $i = h, \Sigma^0$  in the  $h\Sigma^0$  c.m. system and  $\zeta$  is the uniformly distributed cosine of the angle between the vectors  $\mathbf{p}_D$  and  $\mathbf{K}$ .

Since the decay momentum in the  $\Sigma^0 \rightarrow \Lambda\gamma$  is rather small, the velocity of the decay- $\Lambda$  is close to the parent ( $\Sigma^0$ ) velocity and so a substantial part of the  $h\Sigma^0$  correlation at small relative  $h-\Sigma^0$  velocities is transferred to the  $h\Lambda$  correlation at small  $h-\Lambda$  relative velocities. More quantitatively, it follows from Eq. (5) that the parent correlation effect at  $K \approx 0$  of a width  $\Delta K$  yields the  $h\Lambda$  residual correlation effect at  $\langle k^* \rangle \approx p_D m_h / (m_h + m_\Lambda)$  of a width comparable with  $\Delta K$ . Actually, for  $p_D \ll K \ll m_i, m$ , the momentum  $k^*$  is practically independent of  $\zeta$ :  $k^* \approx K(m/m_\Sigma)(m_h + m_\Sigma)/(m_h + m)$  and so, for  $m \approx m_h \approx m_\Sigma$  the residual correlation function recovers the parent one for  $p_D \ll k^* \ll m$ .

As for the transfer of the  $h\Sigma^0$  correlation at small relative velocities to the  $h\gamma$  correlation, the latter is shifted to  $\langle k^* \rangle = p_D / (1 + 2p_D/m_h)^{1/2}$  with the relative width  $\Delta k^* / \langle k^* \rangle \approx \Delta K / [\sqrt{3}\mu_{h\Sigma}(1 + p_D/m_h)]$ , where  $\mu_{h\Sigma} = m_h m_\Sigma / (m_h + m_\Sigma)$  is the reduced mass of the  $h\Sigma^0$ -system. For example, if the hadron  $h$  were a pion or a proton, the residual correlation effects would be respectively situated at  $k^* \approx 34.8$  and  $68 \text{ MeV}/c$  with the corresponding relative

widths  $\Delta K/(332\text{MeV}/c)$  and  $\Delta K/(981\text{MeV}/c)$  much smaller than unity provided that the parent correlation width  $\Delta K$  is less than  $\sim 100 \text{ MeV}/c$ .

## B. Single-channel approach

In the following we will take the hadron  $h$  to be a proton. We thus have to calculate the FSI correlation functions for the systems  $ab = p\Lambda$  and  $p\Sigma^0$  (the FSI between direct photons and protons can be neglected). The two-particle correlation function at small  $k^*$ -values is basically given by the square of the wave function of the corresponding elastic transition  $ab \rightarrow ab$  averaged over the distance  $\mathbf{r}^*$  of the emitters in the two-particle c.m. system and over the particle spin projections [7]:

$$\begin{aligned} \mathcal{R}(\mathbf{p}_1, \mathbf{p}_2) &\doteq \langle |\psi_{-\mathbf{k}^*}^{S(+)}(\mathbf{r}^*)|^2 \rangle \\ &\doteq 1 + \sum_S \rho_S \left[ \frac{1}{2} \left| \frac{f^S(k^*)}{r_0} \right|^2 + \frac{2\Re f^S(k^*)}{\sqrt{\pi}r_0} F_1(Qr_0) - \frac{\Im f^S(k^*)}{r_0} F_2(Qr_0) \right], \end{aligned} \quad (6)$$

where  $F_1(z) = \int_0^z dx e^{x^2 - z^2}/z$  and  $F_2(z) = (1 - e^{-z^2})/z$  and  $\rho_S$  is the emission probability of the two particles in a state with the total spin  $S$ ; we assume the emission of unpolarized particles, i.e.  $\rho_0 = 1/4$  and  $\rho_1 = 3/4$  for pairs of spin-1/2 particles. The analytical expression in Eq. (6) corresponds to the Gaussian  $\mathbf{r}^*$ -distribution (4). It implies a small radius of the FSI interaction as compared with the characteristic separation of the emitters in the two-particle c.m. system. The non-symmetrized wave function describing the elastic transition can then be approximated by a superposition of the plane and spherical waves, the latter being dominated by the s-wave,

$$\psi_{-\mathbf{k}^*}^{S(+)}(\mathbf{r}^*) \doteq \exp(-i\mathbf{k}^*\mathbf{r}^*) + f^S(k^*) \frac{\exp(ik^*r^*)}{r^*}. \quad (7)$$

The s-wave scattering amplitude

$$f^S(k^*) = \frac{\eta^S \exp(2i\delta^S) - 1}{2ik^*} = (1/K^S - ik^*)^{-1}, \quad (8)$$

where  $0 \leq \eta^S \leq 1$  and  $\delta^S$  are respectively the elasticity coefficient and the phase shift,  $K^S$  is a function of the kinetic energy, i.e. an even function of  $k^*$ . In the effective range approximation,

$$1/K^S \doteq 1/a^S + \frac{1}{2}d^S k^{*2}, \quad (9)$$

where  $a^S$  and  $d^S$  are respectively the s-wave scattering length and effective radius at a given total spin  $S$ ; in difference with the traditional definition of the two-baryon scattering length, we follow here the same sign convention as for meson-baryon or two-meson systems.

One can introduce the leading correction  $\mathcal{O}(|a^S|^2 d^S / r_0^3)$  to the correlation function in Eq. (6) to account for the deviation of the wave function (7) from the true solution inside the range of the two-particle strong interaction potential [7]:

$$\Delta\mathcal{R}(\mathbf{p}_1, \mathbf{p}_2) = -(4\sqrt{\pi}r_0^3)^{-1} \sum_S \rho_S |f^S(k^*)|^2 d^S(k^*), \quad (10)$$

where the function  $d^S(k^*) = 2\Re d(K^S)^{-1} / dk^{*2}$ ;  $d^S(0)$  is the effective radius.

It should be noted that the two particles are generally produced at non-equal times in their c.m. system and that the wave function in Eq. (6) should be substituted by the Bethe-Salpeter amplitude. The latter depends on both space ( $\mathbf{r}^*$ ) and time ( $t^*$ ) separation of the emission points in the pair rest frame and at small  $|t^*|$  coincides with the wave function  $\psi^S$  up to a correction  $\mathcal{O}(|t^* / mr^{*2}|)$ , where  $m$  is the mass of the lighter particle. It can be shown that the equal-time approximation in Eq. (6) is usually valid better than to few percent even for particles as light as pions [7, 8].

In this paper we use the low-energy scattering parameters for hyperon-nucleon systems obtained within the spin-flavour  $SU_6$  quark model including effective meson exchange potentials and explicit flavour symmetry breaking of the quark Hamiltonian to reproduce the properties of the two-nucleon system and the low-energy hyperon-nucleon cross section data [6].

The  $K^S$ -function and the low energy scattering parameters are real in the case of only one open channel as in the near threshold  $p\Lambda$  scattering. For  $p\Lambda$  system, we use the values from Table 6 of Ref. [6]:  $a^0 = 2.59$  fm,  $a^1 = 1.60$  fm,  $d^0 = 2.83$  fm and  $d^1 = 3.00$  fm.

For  $p\Sigma^0$  system near threshold, there are two more open channels,  $n\Sigma^+$  and  $p\Lambda$  ones, so, in principle, one has to solve the three-channel scattering problem. Assuming isospin conservation, this problem reduces to the single-channel one for isospin  $I = 3/2$  and to the two-channel one for isospin  $I = 1/2$ . The  $N\Sigma(I = 3/2)$  scattering parameters  $a_I^S$  and  $d_I^S$  are given in Table 6 of Ref. [6]:  $a_{3/2}^0 = 2.51$  fm,  $a_{3/2}^1 = -0.73$  fm,  $d_{3/2}^0 = 4.92$  fm and  $d_{3/2}^1 = -1.22$  fm. The coupling between the channel  $N\Sigma(I = 1/2, S = 0)$  and the  $N\Lambda$  channels appears to be quite weak, i.e. the elasticity coefficient  $\eta^0(k^*) \doteq 1$ , so the low-energy scattering parameters for the  $N\Sigma(I = 1/2, S = 0)$  are real; in accordance with Eq. (8), the



fit of the energy dependence of the  $N\Sigma(I = 1/2, S = 0)$  phase shift in figure 15 (fss2) of Ref. [6] yields  $a_{1/2}^0 = -1.1$  fm and  $d_{1/2}^0 = -1.5$  fm. The situation is quite different for the channel  $N\Sigma(I = 1/2, S = 1)$  which appears to be strongly coupled with the  $N\Lambda$  channels (due to the pion exchange potential) as demonstrated by figures 15 and 31 of Ref. [6]. As a result, the low-energy scattering parameters for the system  $N\Sigma(I = 1/2, S = 1)$  acquire imaginary parts:  $a_{1/2}^1 = (-1.1 + i4.3)$  fm,  $d_{1/2}^1 = (-2.2 - i2.4)$  fm. To get these values, we have used the fact that the  $K$ -function is even in  $k^*$  and employed the expansions corresponding to the effective range approximation in Eq. (9):

$$\begin{aligned}
\eta(k^*) &\doteq 1 - 2\Im a k^* + 2(\Im a)^2 k^{*2} + \left[ 2(\Re a)^2 \Im a - 2(\Im a)^3 - \Im d (\Im a)^2 \right. \\
&\quad \left. + \Im d (\Re a)^2 + 2\Re d \Re a \Im a \right] k^{*3} + \left[ -4(\Re a)(\Im a)^2 + 2(\Im a)^4 \right. \\
&\quad \left. - 4\Re d \Re a (\Im a)^2 + 2\Im d (\Im a)^3 - 2\Im d (\Re a)^2 \Im a \right] k^{*4}, \\
\delta(k^*) &\doteq \delta(0) + \Re a k^* + \left[ -\frac{4}{3}(\Re a)^3 + \Re a (\Im a)^2 + \frac{1}{2}\Re d (\Im a)^2 \right. \\
&\quad \left. + \Im d \Re a \Im a - \Re d (\Re a)^2 \right] k^{*3} + \left[ -2(\Re a \Im a \left( (\Re a)^2 + (\Im a)^2 \right) \right. \\
&\quad \left. + \Re d (\Im a)^3 - \Im d (\Re a)^3 - \Re a \Im a (\Im d \Im a + \Re d \Re a) \right] k^{*4}, \tag{11}
\end{aligned}$$

where  $\delta(0) = 0$  or  $\pm\pi$ . Note however that, due to a rapid fall of the elasticity coefficient and the phase shift near the laboratory  $\Sigma$ -momentum of  $\sim 100$  MeV/ $c$ , the use of the effective range approximation in Eq. (9) is valid up to  $k^*$  of  $\sim 50$  MeV/ $c$  only.

In Fig. 2, we show the  $N\Sigma$  correlation functions corresponding to isospin 3/2 (panel **a**) and 1/2 (panel **b**) as well as the singlet ( $S = 0$ ) and triplet ( $S = 1$ ) contributions calculated according to Eq. (6) for the Gaussian radius  $r_0 = 3$  fm. The enhancement and suppression at small  $k^*$  is related with the positive and negative real parts of the scattering lengths, respectively. A wide suppression of the triplet contribution to the isospin-1/2 correlation function is due to large imaginary parts of the corresponding scattering length and effective radius. Though the effective range approximation is valid for this channel up to  $\sim 50$  MeV/ $c$ , we do not expect a substantial change of the suppression form since at higher values of  $k^*$  the correlation function already starts to approach unity. In any case, one may not rely on the effective range approximation in Eq. (9) and express the scattering amplitude directly through the elasticity coefficient and the phase shift according to Eq. (8).

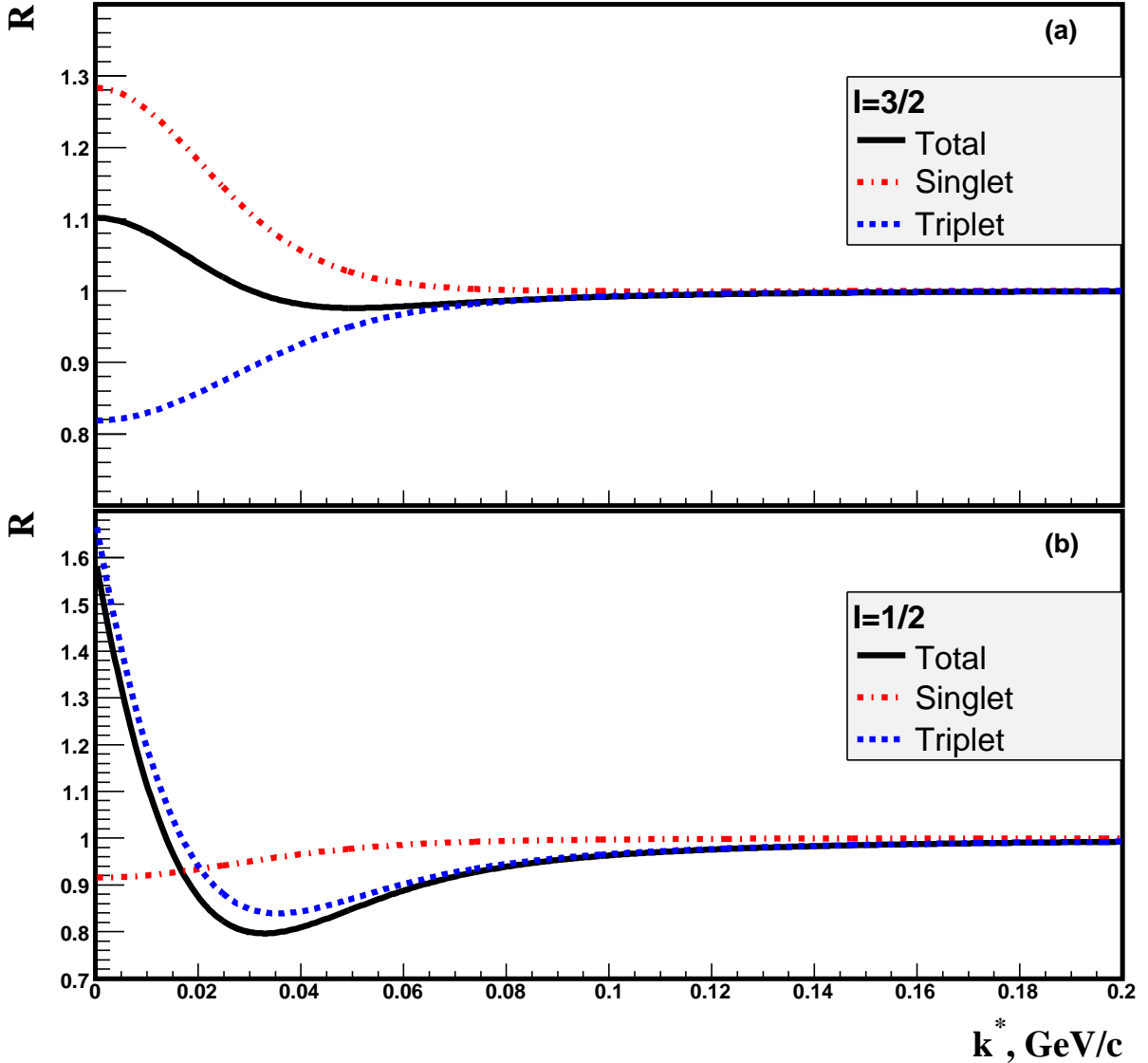


FIG. 2: The  $N\Sigma$  correlation functions corresponding to isospin 3/2 (panel **a**) and 1/2 (panel **b**) calculated for the Gaussian radius  $r_0=3$  fm assuming a uniform population of the spin states, i.e.  $\rho_0 = 1/4$  and  $\rho_1 = 3/4$ . The singlet ( $S = 0$ ) and triplet ( $S = 1$ ) contributions are shown by the dashed-dotted and dashed curves, respectively.

### C. Two-channel approach

The interaction of final state particles  $a$  and  $b$  can proceed not only through the elastic transition  $ab \rightarrow ab$  but also through inelastic reactions of the type  $cd \rightarrow ab$ , where  $c$  and  $d$  are also final state particles of the production process. The FSI effect on particle correlations is

known to be significant only for particles with a slow relative motion. Such particles continue to interact with each other after leaving the domain of particle production and their slow relative motion guarantees the possibility of the separation (factorization) of the amplitude of a slow FSI from the amplitude of a fast production process. For the relative motion of the particles involved in the FSI to be slow, the sums of the particle masses in the entrance and exit channels should be close to each other. Thus, in our case, one should account for the effect of inelastic transition  $n\Sigma^+ \rightarrow p\Sigma^0$  in addition to the elastic transition  $p\Sigma^0 \rightarrow p\Sigma^0$ . Instead of a single channel Schrödinger equation one should thus solve a two-channel one (the effect of the  $p\Lambda$  channel is taken into account in the complex effective single-channel  $K_I$ -functions in the isospin basis). In solving the standard scattering problem, one should take into account that the FSI problem corresponds to the inverse direction of time. As a result, one has to make the substitution  $\mathbf{k}^*(\equiv \mathbf{k}_a^* = -\mathbf{k}_b^*) \rightarrow -\mathbf{k}^*$  and consider  $p\Sigma^0(\equiv 1)$  as the entrance channel and  $n\Sigma^+(\equiv 2)$  as the exit channel. Further, in single-channel equations (7)-(9), one has to substitute the amplitude  $f^S$ , the  $K^S$ -function, the low-energy scattering parameters  $a^S$ ,  $d^S$  and the momentum  $k^*$  by the corresponding symmetric  $2 \times 2$  matrices  $\hat{f}^S$ ,  $\hat{K}^S$ ,  $\hat{a}^S$ ,  $\hat{d}^S$  and  $\hat{k}$ :

$$\hat{f}^S = [(\hat{K}^S)^{-1} - i\hat{k}]^{-1}, \quad (\hat{K}^S)^{-1} = (\hat{a}^S)^{-1} + \frac{1}{2}\hat{d}^S k^{*2}. \quad (12)$$

The momentum matrix  $\hat{k}$  is diagonal in the channel (particle) basis:  $k_{ji} = k_i \delta_{ji}$ ; in accordance with the energy-momentum conservation in the transitions  $1 \rightarrow i$ ,  $k_1 = k_a^* = k_b^* \equiv k^*$  and

$$k_2 = k_c^* = k_d^* = \left[ 2\mu_2 \left( \frac{k^{*2}}{2\mu_1} + m_a + m_b - m_c - m_d \right) \right]^{1/2}, \quad (13)$$

where  $\mu_1 = m_a m_b / (m_a + m_b)$  and  $\mu_2 = m_c m_d / (m_c + m_d)$  are the reduced masses in the channels  $1 = (a, b)$  and  $2 = (c, d)$ . Finally, the wave function  $\psi^S$  in Eq. (7) should be generalized to the two-channel wave function vector  $\psi^{S,i1}$  describing the transitions  $1 \rightarrow i$ :

$$\psi_{-\mathbf{k}^*}^{S,11}(\mathbf{r}^*) = \exp(-i\mathbf{k}^* \mathbf{r}^*) + f_{11}^S(k^*) \frac{\exp(ik^* r^*)}{r^*}, \quad \psi_{-\mathbf{k}_i^*}^{S,21}(\mathbf{r}^*) = f_{21}^S(k^*) \sqrt{\frac{\mu_2}{\mu_1}} \frac{\exp(ik_2^* r^*)}{r^*}, \quad (14)$$

where  $\mathbf{r}^* = \mathbf{r}_a^* - \mathbf{r}_b^*$  or  $\mathbf{r}_c^* - \mathbf{r}_d^*$  is the spatial separation of the particles in the exit channel.

Since the particles in both channels are members of the same isospin multiplets, one can assume that they are produced with about the same probability. Therefore the correlation function will be simply a sum of the average squares of the wave functions  $\psi_{-\mathbf{k}^*}^{S,11}(\mathbf{r}^*)$  and

$\psi_{-\mathbf{k}^*}^{S,21}(\mathbf{r}^*)$  describing the respective elastic and inelastic transitions [9]. Similar to Eq. (1), one then has:

$$\begin{aligned} \mathcal{R}(\mathbf{p}_1, \mathbf{p}_2) &\doteq \langle |\psi_{-\mathbf{k}^*}^{S,11}(\mathbf{r}^*)|^2 \rangle + \langle |\psi_{-\mathbf{k}^*}^{S,21}(\mathbf{r}^*)|^2 \rangle \\ &\doteq 1 + \sum_S \rho_S \left[ \frac{1}{2} \left| \frac{f_{11}^S(k^*)}{r_0} \right|^2 + \frac{2\Re f_{11}^S(k^*)}{\sqrt{\pi}r_0} F_1(Qr_0) - \frac{\Im f_{11}^S(k^*)}{r_0} F_2(Qr_0) \right] \\ &\quad + \sum_S \rho_S \frac{1}{2} \frac{\mu_2}{\mu_1} \left| \frac{f_{21}^S(k^*)}{r_0} \right|^2, \end{aligned} \quad (15)$$

where the analytical expression in Eq. (15) corresponds to the Gaussian  $\mathbf{r}^*$ -distribution (4); since in our case the momentum  $k_2 > k_1 = k^*$  is real, the contribution of the inelastic transition (the last term in Eq. (15)) merely coincides with the quadratic term in the contribution of the elastic transition after the substitution  $f_{11}^S \rightarrow (\mu_2/\mu_1)^{1/2} f_{21}^S$ .

One should correct Eq. (15) for the deviation of the spherical waves from the true scattered waves in the inner region of the short-range potential. The corresponding correction  $\Delta\mathcal{R}$  is of comparable size to the effect of the second channel [9]. It is represented in a compact form in Eq. (125) of Ref. [8], similar to the single-channel correction in Eq. (10). In our case one has

$$\Delta\mathcal{R}(\mathbf{p}_1, \mathbf{p}_2) = -(4\sqrt{\pi}r_0^3)^{-1} \sum_S \rho_S \left[ |f_{11}^S|^2 d_{11}^S + |f_{21}^S|^2 d_{22}^S + 2\Re(f_{11}^S f_{21}^{S*}) d_{21}^S \right], \quad (16)$$

where  $d_{ij}^S = 2\Re d(\hat{K}^S)_{ij}^{-1}/dk^{*2}$ ; at  $k^* = 0$ ,  $\hat{d}^S$  coincides with the real part of the matrix of effective radii.

Assuming that the isospin violation arises solely from the mass difference of the particles within a given isospin multiplet, one can express the elements of the matrices  $\hat{a}^S$ ,  $\hat{d}^S$ ,  $\hat{K}^S$  or  $(\hat{K}^S)^{-1}$  in the channel basis through the elements of the corresponding diagonal matrices in the representation of total isospin  $I$  (the products of the corresponding Clebsch-Gordan coefficients being  $2/3$ ,  $1/3$  and  $\pm\sqrt{2}/3$ ). Particularly,

$$\begin{aligned} (\hat{K}^S)_{11}^{-1} &= \frac{2}{3}(\hat{K}^S)_{3/2}^{-1} + \frac{1}{3}(\hat{K}^S)_{1/2}^{-1} & (\hat{K}^S)_{22}^{-1} &= \frac{1}{3}(\hat{K}^S)_{3/2}^{-1} + \frac{2}{3}(\hat{K}^S)_{1/2}^{-1} \\ (\hat{K}^S)_{21}^{-1} &= (\hat{K}^S)_{12}^{-1} = \frac{\sqrt{2}}{3} \left[ (\hat{K}^S)_{3/2}^{-1} - (\hat{K}^S)_{1/2}^{-1} \right]. \end{aligned} \quad (17)$$

Knowing the elements of the symmetric matrix  $(\hat{K}^S)^{-1}$ , one can make the explicit inversion of the symmetric matrix  $(\hat{f}^S)^{-1}$  given in Eq. (12) and get the required elements  $f_{ij}^S$  of the

scattering amplitude matrix:

$$\begin{aligned}
Df_{11}^S &= (\hat{f}^S)^{-1}_{22} = (\hat{K}^S)^{-1}_{22} - ik_2 & Df_{21}^S &= -(\hat{f}^S)^{-1}_{21} = -(\hat{K}^S)^{-1}_{21} \\
Df_{22}^S &= (\hat{f}^S)^{-1}_{11} = (\hat{K}^S)^{-1}_{11} - ik_1 \\
D &= \det(\hat{f}^S)^{-1} = (\hat{f}^S)^{-1}_{11}(\hat{f}^S)^{-1}_{22} - [(\hat{f}^S)^{-1}_{21}]^2.
\end{aligned} \tag{18}$$

Note that at the momenta  $k_1 = k^*$  sufficiently larger than the momentum  $k_2 = 44.7$  MeV/ $c$  of the channel  $n\Sigma^+$  at the threshold of the channel  $p\Sigma^0$ , one can neglect the difference between the channel momenta and apply the relations (17) directly to the elements of the amplitude matrix  $\hat{f}^S$ .

#### D. Results

The  $p\Sigma^0$  correlation function as well as the singlet ( $S = 0$ ) and triplet ( $S = 1$ ) contributions calculated for the Gaussian radius  $r_0 = 3$  fm are shown in Fig. 3. As already mentioned in the discussion of Fig. 2, the enhancements at small  $k^*$  are related with the positive real parts of the scattering lengths and a wide suppression of the triplet contribution is due to large imaginary parts of the isospin-1/2 scattering length and effective radius.

In Fig. 4, we compare the  $p\Lambda$  correlation function with the  $p\Sigma^0$  and the residual  $p\Lambda_{\Sigma^0}$  ones calculated at the same conditions. Note that in our model the parent correlation functions are independent of the single particle spectra contrary to the residual correlations. To calculate the latter, we have used the thermal-like distribution (2) with  $T_0 = 168$  MeV/ $c$ . One may see that the  $p\Lambda_{\Sigma^0}$  residual correlation function is quite different from the  $p\Lambda$  one. In accordance with the discussion after Eq. (5), the former is close to the parent  $p\Sigma^0$  correlation function for  $k^* > 70$  MeV/ $c$ . In high energy heavy ion collisions the fraction of  $\Lambda$ 's from  $\Sigma^0$  decay is  $\sim 40\%$ . If the corresponding residual correlation were neglected, the parent  $p\Lambda$  correlation effect would be underestimated thus leading to an overestimation of the source size.

The residual  $p\gamma$  correlation functions resulting from the parent  $p\Sigma^0$  correlation due to the  $\Sigma^0 \rightarrow \Lambda\gamma$  decay calculated for different Gaussian radii of the source are shown in Fig. 5. In accordance with the discussion after Eq. (5), the parent correlation at small relative velocities is shifted to rather narrow  $k^*$ -region centered at  $\sim 70$  MeV/ $c$ . Fig. 5 also demonstrates the sensitivity of the residual correlation effect to the source size.

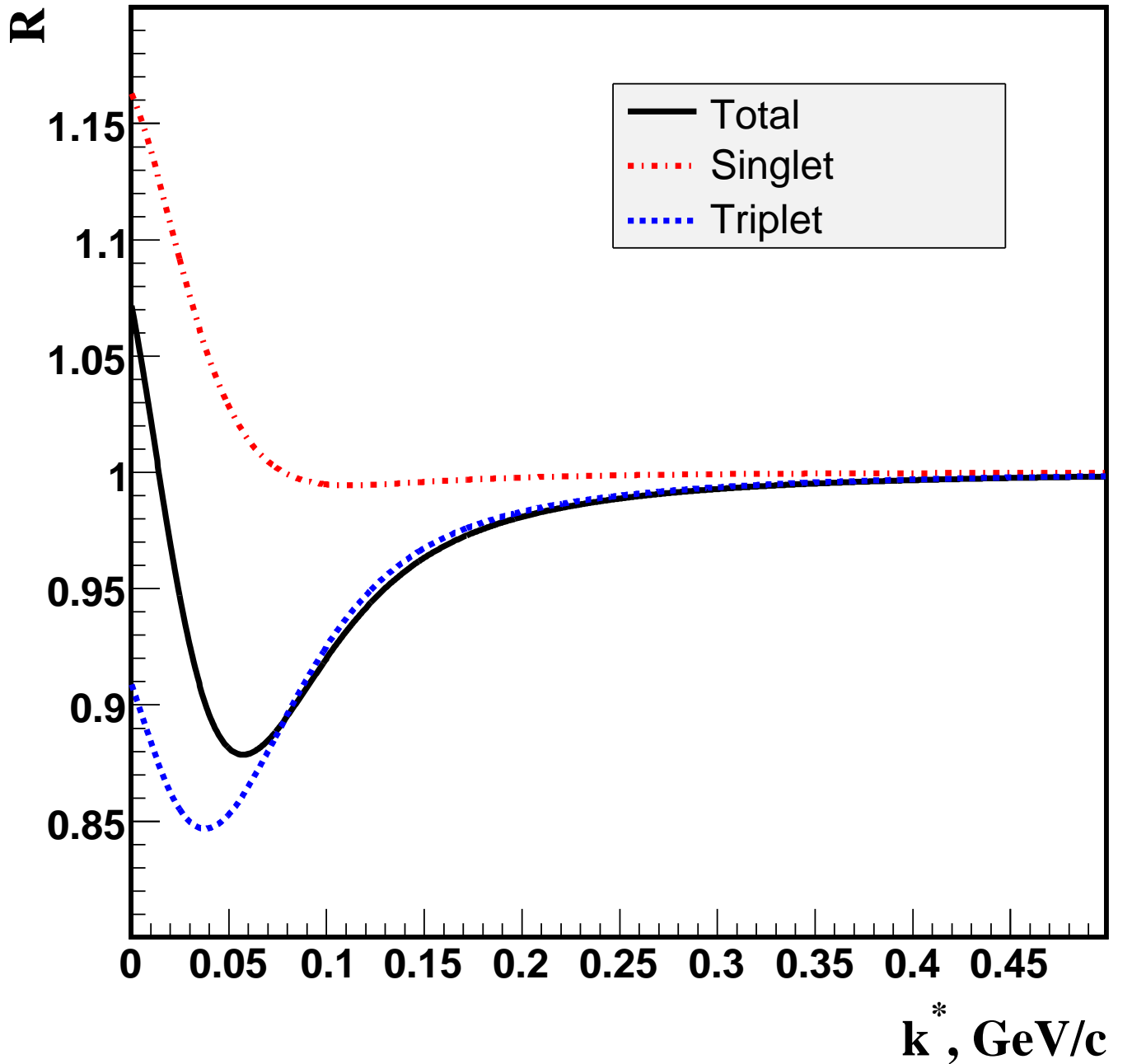


FIG. 3: The  $p\Sigma^0$  correlation function calculated for the Gaussian radius  $r_0=3$  fm assuming a uniform population of the spin states. The singlet ( $S = 0$ ) and triplet ( $S = 1$ ) contributions are shown by the dashed-dotted and dashed curves, respectively.

It should be noted that there exists substantial uncertainty in the theoretical predictions for the low-energy scattering parameters in the isospin-1/2  $N\Sigma$ -channel. Thus the predic-

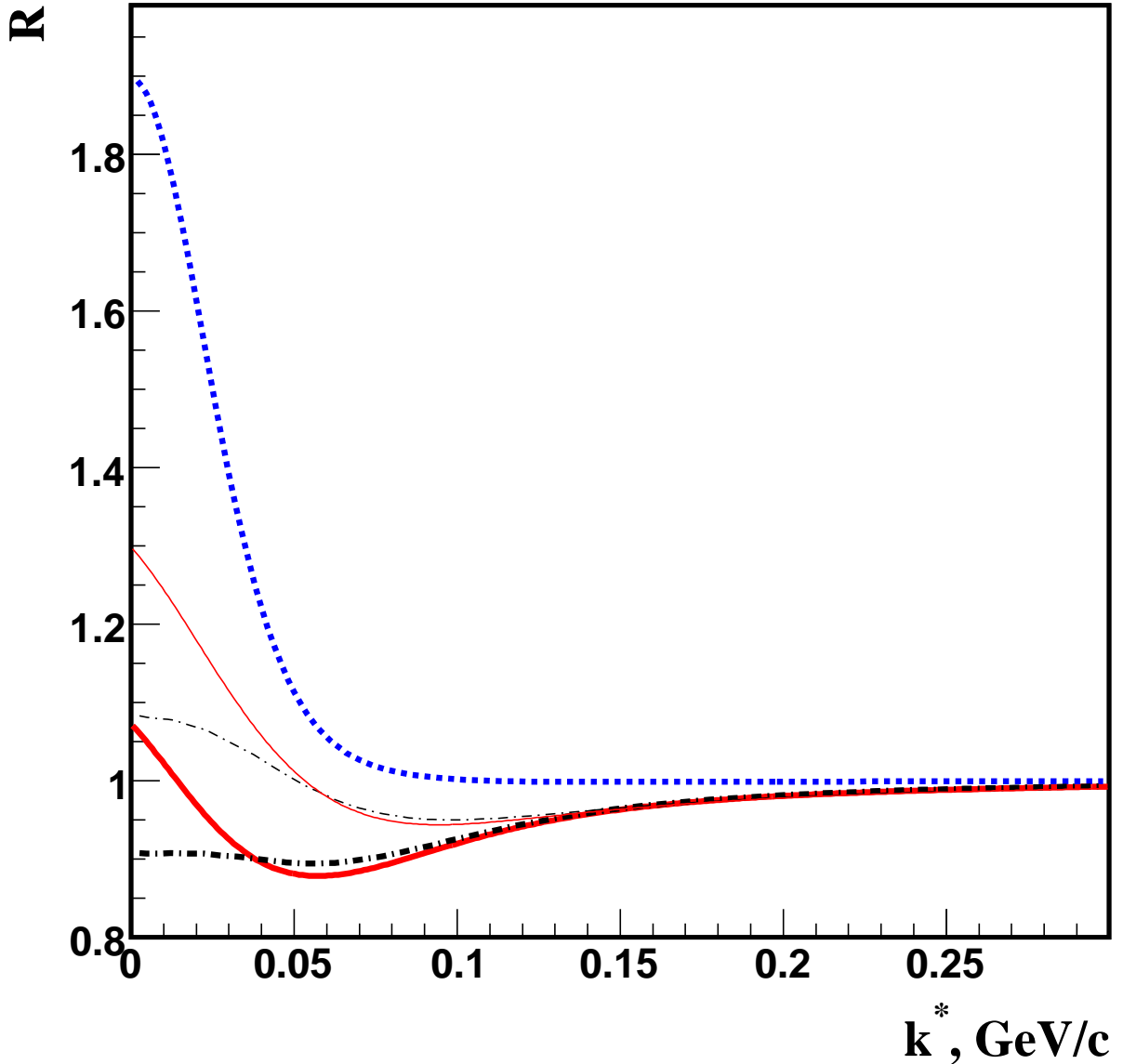


FIG. 4: The  $p\Sigma^0$  (solid curve), the  $p\Lambda$  (dashed curve) and the residual  $p\Lambda_{\Sigma^0}$  (dashed-dotted curve) correlation functions calculated for the Gaussian radius  $r_0=3$  fm assuming a uniform population of the spin states and the thermal-like momentum distribution (2) with  $T_0 = 168$  MeV/c. The thin solid and thin dashed-dotted curves correspond to the  $p\Sigma^0$  and the residual  $p\Lambda_{\Sigma^0}$  correlation functions calculated with the scattering parameters  $a_{1/2}^1 = (2.54 + i0.26)$  fm,  $d_{1/2}^1 = 0$  obtained from the pole position in the NSC89 model [10] on the assumption of vanishing effective radius.

tions of various Nijmegen potential models for the near-threshold pole position  $\alpha_{1/2}^1$  in this channel [10] yield in the limit of zero effective radius, when  $a_{1/2}^1 = \alpha_{1/2}^{1*}/|\alpha_{1/2}^1|^2$ , similar triplet

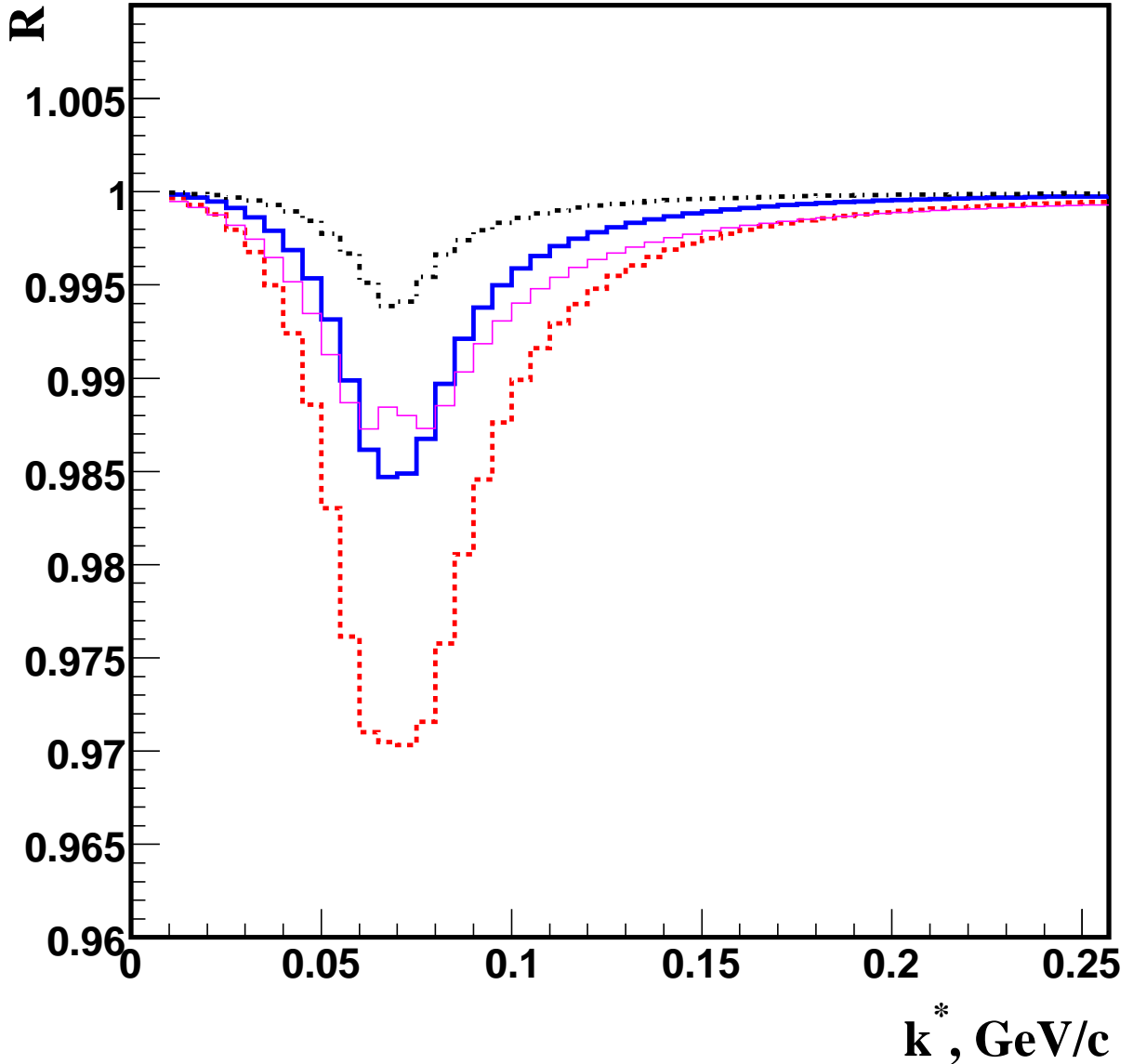


FIG. 5: The residual  $p\gamma\Sigma^0$  correlation function resulting from the parent  $p\Sigma^0$  correlation due to the  $\Sigma^0 \rightarrow \Lambda\gamma$  decay calculated for the Gaussian source radius  $r_0 = 2$  fm (dashed curve),  $r_0 = 3$  fm (solid curve) and  $r_0 = 5$  fm (dashed-dotted curve). The thermal-like momentum distribution (2) with  $T_0 = 168$  MeV/ $c$  is assumed for parent particles. The thin solid curve corresponds to  $r_0 = 3$  fm and the scattering parameters  $a_{1/2}^1 = (2.54 + i0.26)$  fm,  $d_{1/2}^1 = 0$  obtained from the pole position in the NSC89 model [10] on the assumption of vanishing effective radius.

scattering length  $a_{1/2}^1$  as that deduced from Ref. [6] in the case of NSC97f and NF potentials while, they yield even opposite sign of the real part of this scattering length in the case of



earlier NSC89 and ND potentials [11]. To demonstrate the effect of possible uncertainty, we present in figures 4 and 5, besides the correlation functions corresponding to the potential model of Ref. [6], also those obtained from the pole position in the NSC89 model assuming  $d_{1/2}^1 = 0$  [11]:  $a_{1/2}^1 = (2.54 + i0.26)$  fm. One may conclude from these figures that the shape and the intensity of the  $p\Lambda_{\Sigma^0}$  and  $p\gamma_{\Sigma^0}$  residual correlations are sensitive to the  $p\Sigma^0$  FSI and source size parameters thus providing a new possibility to learn about these parameters.

The fraction of residual  $p\gamma$  correlations arising from parent  $p\Sigma^0$  correlations with respect to all other contributions into  $p\gamma$  system is not so large as for the  $p\Lambda$  system. The background arises mainly from photons from  $\pi^0$  decay. Such photons can reduce the effect of our interest in  $p\gamma$  system and make it invisible. The methods of the background suppression depend on experimental details and should be discussed separately.

#### IV. CONCLUSION

The two-photon and proton-photon residual correlations can serve as a new important source of information on the FSI and/or source size parameters as well as on the direct particle fractions. Particularly, a nontrivial femtoscopic irregularity in the proton-photon correlation function centered at  $k^* \approx 70$  MeV/ $c$  is expected due to the  $p\gamma_{\Sigma^0}$  residual correlation. It is shown that the  $p\Lambda_{\Sigma^0}$  residual correlation recovers the negative parent  $p\Sigma^0$  correlation function for  $k^* > 70$  MeV/ $c$ . The neglect of this negative residual correlation would lead to the underestimation of the parent  $p\Lambda$  correlation effect and to an overestimation of the source size.

**Acknowledgements** This work was supported by the RosAtom, the Grant of the Russian Foundation for Basic Research under Contract No. 04-02-17468a and 06-08-01555a, the Grant Agency of the Czech Republic under contract 202/07/0079 and partly carried out within the scope of the GDRE: Heavy ions at ultrarelativistic energies - a European Research Group comprising IN2P3/CNRS, EMN, University of Nantes, Warsaw University of Technology, JINR Dubna, ITEP Moscow and BITP Kiev.

---

[1] R. Lednicky, Phys. Atom. Nucl. **67**, 72 (2004); Nucl. Phys. **A774**, 189 (2006).

- [2] M. Lisa, S. Pratt, R. Soltz and U. Wiedemann, *Ann. Rev. Nucl. Part. Sci.* **55**, 357 (2005).
- [3] D. Peressounko, *Phys. Rev.* **C67**, 014905 (2003).
- [4] M.M. Aggarwal *et al.* (WA98 collaboration), *Phys. Rev. Lett.* **93**, 022301 (2004).
- [5] F. Wang, *Phys. Rev.* **C60**, 067901 (1999); A.V. Stavinskiy *et al.*, *Nucleonika* **49**, suppl.2, s23 (2004).
- [6] Y. Fujiwara, Y. Suzuki and C. Nakamoto, *nucl-th/0607013* (2006).
- [7] R. Lednicky and V.L. Lyuboshitz, *Sov. J. Nucl. Phys.* **35**, 770 (1982); *Proc. CORINNE 90*, Nantes, France, 1990 (ed. D. Ardouin, World Sci., 1990) p. 42.
- [8] R. Lednicky, *nucl-th/0501065*.
- [9] R. Lednicky, V.V. Lyuboshits, and V.L. Lyuboshits, *Phys. At. Nucl.* **61**, 2950 (1998).
- [10] K. Miyagawa and H. Yamamura, *nucl-th/9904002*.
- [11] B. Kerbikov, private communication.